Time-Hopping SSMA Techniques for Impulse Radio with an Analog Modulated Data Subcarrier

Moe Z. Win, Robert A. Scholtz, and Larry W. Fullerton

Abstract – *A time-hopping spread-spectrum communication system employing impulse signal technology has several features which may make it attractive for multiple access communications. These features are outlined and emerging design issues are described. Under ideal propagation conditions, multiple-access capability is estimated for such a communications system with analog frequency shift keyed modulations.*

I. Introduction

There has been tremendous interest in wideband communications systems for personal and cellular communications. Wideband systems offer several advantages over narrowband systems. Some of the attractive features are:

- Wideband systems provide superior ability to operate against several forms of interference, such as multipath, multi-user interference, and narrowband interference;
- Wideband systems allow considerable flexibility in the number of assigned users for a given channel;
- Wideband systems have the ability to operate in an electromagnetic spectrum that is already occupied by other narrowband users without degrading the performance of these existing users;
- Implementation costs of wideband systems have been substantially reduced by advances in communications electronics technology; etc.

The current emphasis in wideband systems has been on constant-envelope spread spectrum modulations. Unfortunately, this ignores one design which has considerable potential, namely time-hopping. The technology for generating and receiving pulses on the order of a nanosecond or less in width, with a shape similar to one cycle of a sine wave, is currently available. These *monocycles* can be received by correlation detection virtually at the antenna terminals, making a relatively low cost receiver possible.

A wideband radio frequency (RF) communication system with time-hopping spread-spectrum modulation format is described in this paper. This wideband communication system is referred to as an *impulse radio* because it utilizes the available impulse signal technology in which the information carrying waveform is an extremely narrow pulse. This impulse radio has several features which may make it attractive for multiple access communications. These features are outlined and an estimate of the multiple-access capability of the impulse radio under ideal propagation conditions is presented.

The research described in this paper was supported in part by the Joint Services Electronics Program under contract F49620-94-0022

Moe Z. Win and Robert A. Scholtz are with Communication Sciences Institute, Department Electrical Engineering-Systems, University of Southern California, Los Angeles, CA 90089-2565 USA.

Larry W. Fullerton is with Time Domain Systems, Inc. 6700 Odyssey Drive, Suite 100, Huntsville, AL 35806 USA.

The primary author can be reached at win@milly.usc.edu

II. Time-Hopping Format Using Impulses

A typical time-hopping format employed by an impulse radio in which the $k^{\underline{\text{th}}}$ transmitter's output signal $s_{\text{tr}}^{(k)}(u, t^{(k)})$ is given by

$$s_{\text{tr}}^{(k)}(u, t^{(k)}) = \sum_{j=-\infty}^{\infty} w_{\text{tr}}(t^{(k)} - jT_{\text{f}} - c_j^{(k)}(u)T_{\text{c}} - d_j^{(k)}(u)), \tag{1}$$

where $t^{(k)}$ is the transmitter's clock time. Here $w_{\text{tr}}(t)$ represents the transmitted monocycle waveform that nominally begins at time zero on the transmitter's clock, and the quantities associated with (k) are transmitter dependent. Hence the signal emitted by the $k^{\underline{\text{th}}}$ transmitter consists of a large number of monocycle waveforms shifted to different times, the $j^{\underline{\text{th}}}$ monocycle nominally occurring at time $jT_{\text{f}} + c_j^{(k)}(u)T_{\text{c}} + d_j^{(k)}(u)$. The structure of each time shift component is described in detailed as follows:

(A) Uniform Pulse Train Spacing: A pulse train of the form $\sum_{j=-\infty}^{\infty} w_{\text{tr}}(t^{(k)} - jT_{\text{f}})$ consists of monocycle pulses spaced T_{f} seconds apart in time. The *frame time* or *pulse repetition time* typically may be a hundred to a thousand times the monocycle width, with its largest value constrained in part by the stability of the available clocks. The result is a signal with a very low duty cycle. Multiple-access signals composed of uniformly spaced pulses are vulnerable to occasional *catastrophic collisions* in which a large number of pulses from two signals are received simultaneously, much as might occur in spread ALOHA systems [1].

(B) Random/Pseudorandom Time-Hopping: To eliminate catastrophic collisions in multiple accessing, each user (indexed by k) is assigned a distinct pulse shift pattern $\{c_j^{(k)}(u)\}$ called *a time-hopping code*. These hopping codes $\{c_j^{(k)}(u)\}$ are pseudorandom with period N_{p}, i.e., $c_{j+iN_{\text{p}}}(u) = c_j(u)$ for all integers j and i. Each element of the time-hopping sequence $\{c_j^{(k)}(u)\}$ is an integer in the range $0 \le c_j^{(k)}(u) < N_{\text{h}}$. The time-hopping code therefore provides an additional time shift to each pulse in the pulse train, with the $j^{\underline{\text{th}}}$ monocycle undergoing an added shift of $c_j^{(k)}(u)T_{\text{c}}$ seconds. Hence the additional time shifts caused by the code are discrete values between 0 and $N_{\text{h}}T_{\text{c}}$ seconds.

It is assumed that $N_{\text{h}}T_{\text{c}} \le T_{\text{f}}$, and hence the ratio $N_{\text{h}}T_{\text{c}}/T_{\text{f}}$ indicates the fraction of the frame time T_{f} over which time-hopping is allowed. Since a short time interval is required

to read the output of a monocycle correlator and to reset the correlator, it is assumed that $N_h T_c/T_f$ is strictly less than one. If $N_h T_c/T_f$ is too small, then catastrophic collisions remain a significant possibility. Conversely, with a large enough value of $N_h T_c/T_f$ and well designed codes, the multiple access interference in many situations can be modeled as a Gaussian random process [2].

Since the hopping code is periodic with period N_p, the waveform $\sum_{j=-\infty}^{\infty} w_{tr}(t^{(k)} - jT_f - c_j^{(k)}(u)T_c)$ is periodic with period $T_p = N_p T_f$. It can be shown that the time-hopping code effectively reduces the power spectral density (PSD) of the uniformly spaced pulse train from a line spectral density ($1/T_f$ apart) down to a spectral density with finer lines $1/T_p$ apart.

(C) Data Modulation: The sequence $\{d_j^{(k)}(u)\}_{j=-\infty}^{\infty}$ is a sample sequence from a wide-sense stationary random process $d^{(k)}(u,t)$, with samples taken at a rate of T_f^{-1}. For an analog frequency shift keyed (FSK) data subcarrier, $d^{(k)}(u,t)$ can be written as

$$d^{(k)}(u,t) = K \sum_n \lceil \overline{T_s} \rceil (t - nT_s) \cos[2\pi(f_c + \Delta f_n(u))t + \theta(u)] . \quad (2)$$

The rectangle function is defined by

$$\lceil \overline{T} \rceil (t) \triangleq \begin{cases} 1 & \text{for} \quad |t| < T/2 \\ 0 & \text{otherwise,} \end{cases} \quad (3)$$

and K is a scaling constant whose significance will be discussed later. The random variable $\theta(u)$ is uniformly distributed on the interval $[-\pi, \pi)$.

In the case of binary FSK, the carrier frequency f_c is shifted by $\Delta f_n(u) = f_0$ or $\Delta f_n(u) = f_1$ depending upon whether the n^{th} data symbol is zero or one, respectively. This form of modulation is of particular interest for low power or miniaturized applications. Other forms of modulation can be employed to benefit the performance of synchronization loops, interference rejection, implementation complexity, etc. Of course, the data modulation further smoothes the PSD of the pseudo random time-hopping signal.

In this modulation format, a single symbol has a duration $T_s = N_s T_f$. For a fixed frame (pulse repetition) time T_f, the *binary symbol rate* R_s determines the number N_s of monocycles that are modulated by a given binary symbol, via the equation

$$R_s = \frac{1}{T_s} = \frac{1}{N_s T_f} \text{ sec.}^{-1} \quad (4)$$

III. The Channel Model

When N_u users are active in the multiple-access system, the composite received signal $r(u,t)$ at the output of this receiver's antenna is modelled as

$$r(u,t) = \sum_{k=1}^{N_u} A_k s_{rec}^{(k)}(u, t - \tau_k(u)) + n(u,t) , \quad (5)$$

in which A_k models the attenuation over the propagation path of the signal $s_{rec}^{(k)}(u, t - \tau_k(u))$ received from the k^{th} transmitter. The random variable $\tau_k(u)$ represents the time asynchronisims between the clocks of transmitter k and the receiver,

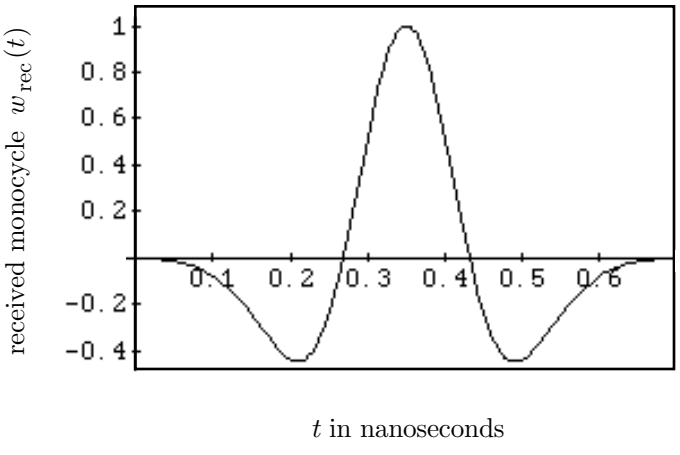

Figure 1: The received monocycle $w_{rec}(t)$ at the output of the antenna subsystem as a function of time in nanoseconds.

and $n(u,t)$ represents other non-monocycle interference (e.g., receiver noise) present at the correlator input.

The above model may seem rather simple at first glance, but let's enumerate and expound on some of the assumptions that are implicit in this model. The following are assumed to hold over the duration of a data symbol that the central receiver is trying to decode.

(a) *Identically Formatted Transmissions:* The waveforms $s_{tr}^{(k)}(u, t^{(k)})$, $k = 1, 2, \ldots, N_u$, are identical in time scale and format, differing only in the time-hopping code and data modulation that are used in their construction. The quantity $t^{(k)}$ here refers to time as measured by the k^{th} transmitter's clock.

(b) *Common-Frequency Clocks:* The quantity t represents time as measured by a clock at the central node's receiver. Assume further that all the transmitters' clocks tick at the same rate (e.g., they may be derived by time-transfer techniques from a clock signal that is broadcast by the central node), and from the central receiver's viewpoint, $t^{(k)}$ differs from the central receiver's clock by a random time offset $\tau_k(u)$, i.e., $\tau_k(u) = t - t^{(k)}(u)$. The statistics of $\tau_k(u)$ generally are determined by how the clock signals of the different receivers are derived.

(c) *Short-Term Constant Parameters:* The number of transmitters N_u on the air is assumed to be constant during the data symbol interval that is being analyzed, and the signal amplitudes A_k are fixed over this same interval.

(d) *Ideal Channel Assumptions:* The propagation of the signals from each transmitter to the central receiver is assumed to be ideal, each signal undergoing only a constant attenuation and delay. The antenna modifies the shape of the transmitted monocycle $w_{tr}(t)$ to $w_{rec}(t)$ at the output of the central receiver's antenna.

The nominal received pulse shape $w_{rec}(t)$ is shown in figure 1, indicating that the pulse approximately occupies the time interval $[0, 0.7]$ nanoseconds (The pulse width is usually limited to 0.7 nanoseconds in later numerical calculations to reduce computation time). Therefore the received signal component from the k^{th} transmitter as a function of the central

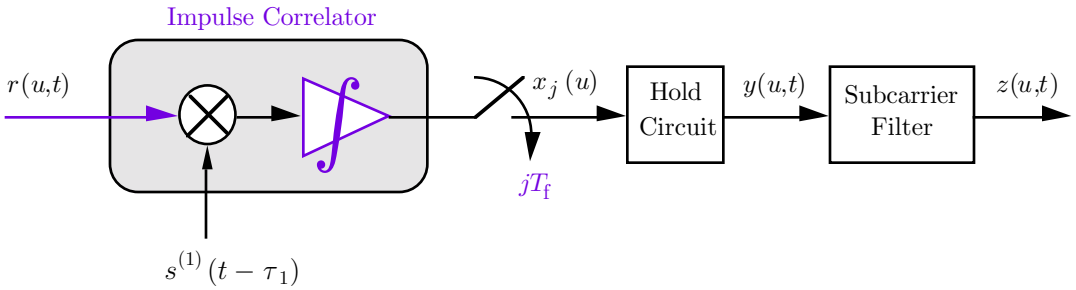

Figure 2: Simplified model of the analog impulse radio multiple access receiver front end.

receiver's clock time t is

$$s_{\mathrm{rec}}^{(k)}(u, t-\tau_k(u)) = \sum_{j=-\infty}^{\infty} w_{\mathrm{rec}}(t-\tau_k(u)-jT_{\mathrm{f}}-c_j^{(k)}(u)T_{\mathrm{c}}-d_j^{(k)}(u))\,. \quad (6)$$

This channel model ignores multipath, dispersive effects, etc.

These assumptions concerning the signal structure and timing are necessary to perform a reasonably simple analysis.

IV. The Analog Impulse Radio Multiple Access Receiver

A simplified model describing a portion of the analog impulse radio multiple access (AIRMA) receiver is shown in figure 2. A more comprehensive description of the AIRMA receiver can be found in [3], where detailed calculations of the mathematical structure at various locations of the AIRMA receiver are made. The results are summarized here with the important assumptions that were made during the calculations.

(e) *Perfect Synchronization*: Assume that the receiver is locked on to the transmission from the first user so that it achieved both clock and code synchronization for the signal transmitted by the first transmitter, i.e., τ_1 and $\{c_j^{(1)}\}$ are no longer random variables from the receiver's viewpoint.

That is, the receiver has determined $\tau_1(u)$ precisely, and has a replica of the first user's time-hopping code running synchronously with the time hops received via the air waves from user 1. Hence the signal on the local reference arm of the receiver correlator, coming from the template generator, is simply

$$s^{(1)}(u, t-\tau_1(u)) = \sum_{j=-\infty}^{\infty} w_{\mathrm{cor}}(t-jT_{\mathrm{f}}-c_j^{(1)}(u)T_{\mathrm{c}}-\tau_1(u))\,, \quad (7)$$

which looks formally like the received waveform from user 1 with no data modulation imposed on it, and with a different pulse shape $w_{\mathrm{cor}}(t)$ in place of the monocycle.

The impulse correlator output is sampled to obtain the sequence $\{x_j(u)\}$, and held by the sample and hold (S/H) device at a rate of one sample per frame. The correlator output corresponding to the $j^{\underline{\mathrm{th}}}$ frame of the user 1 waveform can be expressed by

$$x_j(u) = \int_{-\infty}^{\infty} r(u,t)\, w_{\mathrm{cor}}(t-jT_{\mathrm{f}}-c_j^{(1)}(u)T_{\mathrm{c}}-\tau_1(u))\, dt\,. \quad (8)$$

Note that the range of integration here is actually determined mathematically by the time over which the locally generated pulse $w_{\mathrm{cor}}(t-jT_{\mathrm{f}}-c_i^{(1)}(u)T_{\mathrm{c}}-\tau_1(u))$ is non-zero, and assume that (8) is a reasonable representation for the correlator output sample.

As indicated in figure 2, the impulse correlator output values are sampled to obtain the sequence $\{x_j(u)\}$ and held to create a signal $y(u,t)$. The sample and hold device output is then passed through a subcarrier filter to produce the signal $z(u,t)$ that is to be demodulated. (This description is reasonably accurate for both the voice and data subcarrier processing.)

The subcarrier filter output signal was evaluated in [3] as

$$z(u,t) = z^{(1)}(u,t) + \underbrace{\sum_{k=2}^{N_{\mathrm{u}}} z^{(k)}(u,t) + z_{\mathrm{rec}}(u,t)}_{\triangleq\ z_{\mathrm{noise}}(u,t)}, \quad (9)$$

where $z_{\mathrm{rec}}(u,t)$ accounts for the effects of receiver noise and all other non-monocycle interference. Since the receiver's correlation circuitry is set to receive user 1's signal, $z^{(k)}(u,t)$ for $k = 2, 3, \ldots, N_{\mathrm{u}}$ in (9) represent the interference due to multiple access noise at the demodulator input. The desired input signal to the demodulator is $z^{(1)}(u,t)$ given by

$$z^{(1)}(u,t) = T_{\mathrm{f}}A_1 \sum_{j=-\infty}^{\infty} \widetilde{R}_w(d_j^{(1)}(u))\, g'_{\mathrm{subcar}}(t-jT_{\mathrm{f}}-\gamma)\,, \quad (10)$$

where $\widetilde{R}_w(\tau)$ is the cross-correlation function defined by

$$\widetilde{R}_w(\tau) \triangleq \int_{-\infty}^{\infty} w_{\mathrm{rec}}(t+\tau) w_{\mathrm{cor}}(t)\, dt\,, \quad (11)$$

and γ is a delay on the order of $\tau_1(u) + T_{\mathrm{f}}$ that is of no consequence to the calculations that follow. When $1/T_{\mathrm{f}}$ is much larger than any frequency passed by the subcarrier filter, then $g'_{\mathrm{subcar}}(t) \approx g_{\mathrm{subcar}}(t)$, where $g_{\mathrm{subcar}}(t)$ is the impulse response of the subcarrier filter. In the current designs of the AIRMA receiver, this appears to be a reasonable approximation.

(f) *Ideal Interpolation*: Assume for simplicity that perfect signal reconstruction from the samples takes place, i.e., $g'_{\mathrm{subcar}}(t)$ is the ideal interpolating function for reconstructing the waveform from samples. With a complete knowledge of the information signal's statistics and an acceptable performance criterion, it might be possible to optimally design this filter for signal reconstruction purposes.

Under the assumption of perfect signal reconstruction, $z^{(1)}(u,t)$ has an especially simple form, namely

$$z^{(1)}(u,t) = A_1 \widetilde{R}_w(d^{(1)}(u,t-\gamma')) \approx \dot{\widetilde{R}}(0) d^{(1)}(u,t-\gamma') \quad \text{for small } d^{(1)}(u,\cdot)\,. \tag{12}$$

The parameter $\dot{\widetilde{R}}(0)$ represents the slope of $\dot{\widetilde{R}}(t)$ at $t=0$, $d^{(1)}(u,t)$ represents the transmitted subcarrier signal of user 1 before sampling, and γ' accounts for propagation and processing delays. If the scaling constant K in (2) is such that the data modulation levels are small enough, then $d^{(1)}(u,\cdot)$ always falls in the linear region and the approximation in (12) is reasonable. Figure 3 shows exact and approximate expressions for the cross-correlation function $\widetilde{R}_w(\tau)$. This figure shows that the linear approximation in (12) is reasonable as long as $\tau \leq 0.025$ nanoseconds. Under these ideal circumstances, the modulation $d^{(1)}(u,t)$ is directly visible with little or no distortion at the output of the AIRMA receiver subcarrier filter.

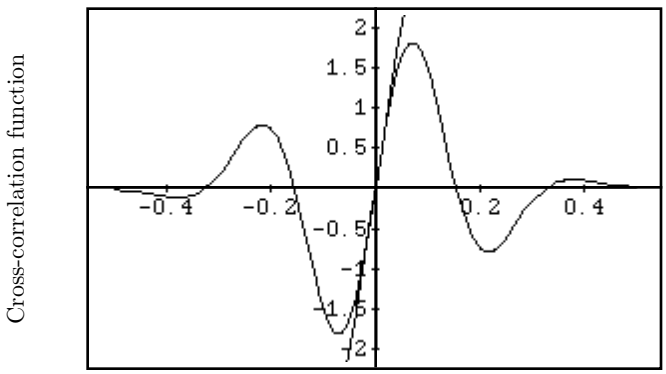

Figure 3: Cross-correlation between the received waveform and pulse correlator waveform. Also shown is the linear approximation of this cross-correlation function.

V. SNR Calulations

The single-user signal-to-noise ratio (SNR) at the output of the subcarrier filter is defined to be

$$SNR_{\text{out}}(1) \triangleq \frac{\langle \mathbb{E}\{|z^{(1)}(u,t)|^2\}\rangle}{\langle \mathbb{E}\{|z_{\text{rec}}(u,t)|^2\}\rangle}\,. \tag{13}$$

The notation $\langle\cdot\rangle$ is used to indicate a time average, in this case over the duration T_{f} of the "hold", to make this measure insensitive to time. The expression for the numerator is evaluated in [3] as

$$\langle \mathbb{E}\{|z^{(1)}(u,t)|^2\}\rangle = \frac{1}{2} A_1^2 (\dot{\widetilde{R}}(0)K)^2\,. \tag{14}$$

The following assumption is made for the random noise sequence because of the lack of further knowledge about the signals that contribute to $n(u,t)$.

(g) Independent Receiver Noise Samples: It is simply assumed that the random noise sequence contributed by the receiver noise at the pulse correlator output is composed of independent random variables with mean zero and variance $\mathbb{E}\{[n_j(u)]^2\} = \sigma_{\text{n}}^2$. This model is reasonable for wideband interference and receiver noise.

The quantity $\langle \mathbb{E}\{|z_{\text{rec}}(u,t)|^2\}\rangle$, the noise power at the output of the subcarrier filter due to receiver noise, is calculated in [3] as

$$\langle \mathbb{E}\{|z_{\text{rec}}(u,t)|^2\}\rangle = 2BT_{\text{f}}\sigma_{\text{n}}^2\,, \tag{15}$$

where B is a one sided noise equivalent bandwidth of the subcarrier filter. Substituting (14) and (15) into (13) gives the single-user SNR at the output of the subcarrier filter to be

$$SNR_{\text{out}}(1) = \frac{A_1^2(\dot{\widetilde{R}}(0)K)^2}{4BT_{\text{f}}\sigma_{\text{n}}^2}\,. \tag{16}$$

When the signals of other users are present and the receiver is synchronized to user 1's transmission, then the signals of other users must be treated as interference. To calculate the effect of multiple-user interference, a randomly coded signal set model is used and independent interference sources assumption is made.

(h) Random Coding: Assume a randomly coded signal set model, in which the hopping code $\{c_j^{(k)}(u)\}$ of each user k is selected independently of the selection of other user's codes. This is a conservative assumption because one would expect to do somewhat better by selecting the codes to minimally interfere with each other, as indeed this is one of the topics for future research.

(i) Independent Interference Sources: Assume that the signals $s_{\text{rec}}^{(k)}(u,t-\tau_k(u))$, for $k=2,3,\ldots,N_{\text{u}}$ and $n(u,t)$ are independently generated. Therefore the received signals from different users are totally asynchronous, and the delay variables $\tau_k(u)$ are independent for different users. Hence, the N_{u} random variables $s_j^{(k)}(u)$, for $k=2,3,\ldots,N_{\text{u}}$, and $n_j(u)$ are independent random variables.

The N_{u}-user SNR at the output of the subcarrier filter is defined to be

$$SNR_{\text{out}}(N_{\text{u}}) \triangleq \frac{\langle \mathbb{E}\{|z^{(1)}(u,t)|^2\}\rangle}{\langle \mathbb{E}\{|z_{\text{noise}}(u,t)|^2\}\rangle}\,. \tag{17}$$

The quantity $\langle \mathbb{E}\{|z^{(1)}(u,t)|^2\}\rangle$ is given previously in (14). The quantity $\langle \mathbb{E}\{|z_{\text{noise}}(u,t)|^2\}\rangle$ is the total noise power at the demodulator input, and is evaluated in [3] as

$$\langle \mathbb{E}\{|z_{\text{noise}}(u,t)|^2\}\rangle = 2BT_{\text{f}}\sigma_{\text{n}}^2 + 2BT_{\text{f}}\sigma_{\text{self}}^2 \sum_{k=2}^{N_{\text{u}}} A_k^2\,, \tag{18}$$

where σ_{self}^2 is defined to be

$$\sigma_{\text{self}}^2 \triangleq T_{\text{f}}^{-1} \int_{-\infty}^{\infty} \left[\int_{-\infty}^{\infty} w_{\text{rec}}(t+\zeta) w_{\text{cor}}(t) dt\right]^2 d\zeta\,. \tag{19}$$

Substituting (14) and (18) into (17), the useful N_{u}-user SNR at the subcarrier filter output becomes

$$SNR_{\text{out}}(N_{\text{u}}) = \frac{\frac{1}{2}A_1^2(\dot{\widetilde{R}}(0)K)^2}{2BT_{\text{f}}\sigma_{\text{n}}^2 + 2BT_{\text{f}}\sigma_{\text{self}}^2 \sum_{k=2}^{N_{\text{u}}} A_k^2}\,. \tag{20}$$

When $N_u = 1$, the second term in the denominator is zero and (20) is reduced exactly to the expression previously derived in (16). It is desirable to rewrite this expression as

$$SNR_{\text{out}}(N_u) = \left\{ SNR_{\text{out}}^{-1}(1) + M_{\text{AIRMA}} \sum_{k=2}^{N_u} \left(\frac{A_k}{A_1} \right)^2 \right\}^{-1} . \quad (21)$$

This structure of N_u-user SNR for general multi-user communications was suggested before [4], and calculated for a direct sequence code division multiple-access system [5]. The parameter M_{AIRMA} is the modulation coefficient of the AIRMA receiver defined by

$$M_{\text{AIRMA}}^{-1} \triangleq \frac{(\dot{\tilde{R}}(0)K)^2}{4BT_f\sigma_{\text{self}}^2} . \quad (22)$$

VI. Performance Measure

In this section, the interpretations of N_u-user SNR derived in the previous sections will be made and related to the performance of the impulse radio in terms of multiple access capacity (MAC). Multiple access capacity is defined as the number of users that multiuser communication system can support for a given level of uncoded bit error probability performance, data rate, and other modulation parameters.

To calculate the performance measure, first rewrite (21) as

$$\sum_{k=2}^{N_u} \left(\frac{A_k}{A_1} \right)^2 = M_{\text{AIRMA}}^{-1} SNR_{\text{out}}^{-1}(N_u) \left\{ 1 - \frac{SNR_{\text{out}}(N_u)}{SNR_{\text{out}}(1)} \right\} . \quad (23)$$

For a specified average bit error probability performance, $SNR_{\text{out}}(N_u)$ can be interpreted as the required SNR at the receiver demodulator in the presence of the other $N_u - 1$ users. If only user 1 were active, then there would be no multiple access interference and the SNR at the input of the receiver demodulator would increase to $SNR_{\text{out}}(1)$. In this case the bit error probability would be clearly reduced from the specified value by as much as several orders of magnitude. Therefore the ratio of $SNR_{\text{out}}(1)$ to $SNR_{\text{out}}(N_u)$ represents the additional amount of power required for user 1, over and above that is needed when only one user is active, to overcome the multiple access interference caused by the presence of $N_u - 1$ other users. It is convenient to define the additional required power, ARP, in dB as

$$APR \triangleq 10 \log_{10} \left\{ \frac{SNR_{\text{out}}(1)}{SNR_{\text{out}}(N_u)} \right\} \quad [\text{dB}]. \quad (24)$$

For the receiver with perfect power control capability, i.e., $A_k = A_1$ for all k, then (23) simplifies to

$$N_u(ARP) = \left\lfloor M_{\text{AIRMA}}^{-1} SNR_{\text{out}}^{-1}(N_u) \left\{ 1 - 10^{-(ARP/10)} \right\} \right\rfloor + 1 , \quad (25)$$

where the number of user is written explicitly as a function of ARP to emphasize its dependence on ARP. The notation $\lfloor z \rfloor$ represents the largest integer less than or equal to z. The limiting value of N_u as ARP approaches to infinity is the maximum theoretical achievable multiple access capacity of the impulse radio. This maximum multiple access capacity is given by

$$MMAC \triangleq \lim_{ARP \to \infty} N_u(ARP) = \lfloor M_{\text{AIRMA}}^{-1} SNR_{\text{out}}^{-1}(N_u) \rfloor + 1 . \quad (26)$$

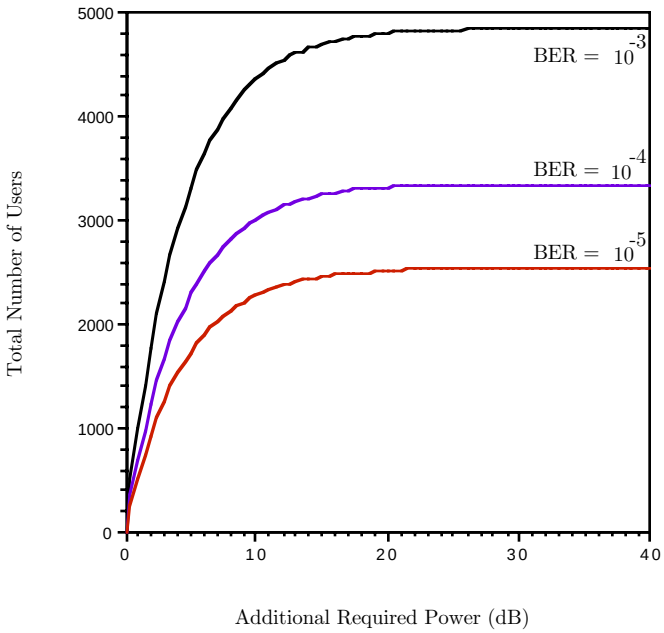

Figure 4: Total number of users versus additional required power (dB) for AIRMA receiver. This figure is plotted for three different performance levels with the data rate of 19.2 Kbps.

Since $MMAC$ is the maximum achievable theoretical limit, it can be used to bound the number of users $N_u(ARP)$ of the impulse radio as $N_u(ARP) \leq MMAC$. This is a striking (but not surprising) result which says that the number of users at a specified bit error rate (BER) can not be larger than $MMAC$ no matter how large the power of each user's signal is. In other words, when the number of active users is more than $MMAC$, then the receiver can not maintain the specified level of performance regardless of the additional available power.

XII. Performance Evaluation

As shown in the previous section the performance of the AIRMA receiver is affected by the choice of modulation parameters only through the quantity M_{AIRMA}. For AIRMA receiver detecting analog FSK modulation with $K = 0.025$, $T_f = 100$ nanoseconds, and data rate $R_s = 19.2$ kbps, M_{AIRMA}^{-1} is evaluated numerically as 4.63×10^4. In this calculation the subcarrier filter bandwidth is set as $2B = 1/T_s$. A larger subcarrier bandwidth is possible but would degrade the system performance since this allows more noise to pass through the filter.

Given these parameters, the number of users versus additional required power for AIRMA is plotted in figure 4 for typical BERs. To maintain BER of 10^{-3}, 10^{-4}, and 10^{-5} in a communications systems with no error control coding, $SNR_{\text{out}}(N_u)$ must be 12.8 dB, 14.4 dB, and 15.6 dB respectively. Note that the number of users increases rapidly as the ARP increases from 0 to 10 dB. However, this improvement becomes gradual as ARP increases from 10 to 20 dB. After this point, only negligible improvement can be made as ARP increases and finally reaches the $MMAC$. In practice, impulse radios are expected to operate in regions where the increase in the number of users as a function of ARP is

rapid. Figure 4 quantitatively provides the trade-off between the number of additional users and the additional power required to maintain the respective BERs. The $MMAC$ for AIRMA is calculated to be 4846, 3353, and 2544 for BER of 10^{-3}, 10^{-4}, and 10^{-5} respectively.

XIII. Conclusions

Under ideal propagation conditions, the total number of users is shown to increase rapidly as additional required power increases. However these improvements become gradual after a certain point and finally reaches the limit which is referred to as maximum multiple access capacity. It can be concluded that if the number of active users is more than $MMAC$, then the receiver can not maintain the specified level of performance regardless of the additional available power. The results obtained in this paper are fairly general and quantitatively provide the trade-off for system design issues.

Acknowledgments

The authors wish to thank Mark Barnes of Time Domain Systems, Inc., and Paul Withington of Pulson Communications for several helpful discussions concerning the technology, capabilities, and signal processing of impulse signals.

References

1. N. M. Abramson, "VSAT Data Networks," *Proc. IEEE*, July 1990, pp. 1267-1274.
2. R. A. Scholtz, "Multiple Access with Time-Hopping Impulse Modulation," *Proc. MILCOM*, Boston, MA, Oct. 11-14, 1993.
3. M. Z. Win, and R. A. Scholtz, "Comparisons of Analog and Digital Impulse Radio for Multiple Access Communications," To be submitted to *IEEE Trans. on Comm.*, In Progress .
4. G. R. Cooper and R. W. Nettleton, "A Spread Spectrum Technique for High-Capacity Mobile Communications," *IEEE Trans. on Vehicular Technology*, vol. VT-27, Nov. 1978, pp. 264-275.
5. C. L. Weber, G. K. Huth, and B. H. Batson, "Performance Considerations of Code Division Multiple-Access Systems," *IEEE Trans. on Vehicular Technology*, vol. VT-30, Feb. 1981, pp. 3-9.